nature neuroscience

Synaptic signaling between GABAergic interneurons and oligodendrocyte precursor cells in the hippocampus

Shih-chun Lin & Dwight E Bergles

Oligodendrocyte precursor cells (OPCs) express receptors for many neurotransmitters, but the mechanisms responsible for their activation are poorly understood. We have found that quantal release of GABA from interneurons elicits $GABA_A$ receptor currents with rapid rise times in hippocampal OPCs. These currents did not exhibit properties of spillover transmission or release by transporters, and immunofluorescence and electron microscopy suggest that interneuronal terminals are in direct contact with OPCs, indicating that these GABA currents are generated at direct interneuron–OPC synapses. The reversal potential of OPC $GABA_A$ currents was –43 mV, and interneuronal firing was correlated with transient depolarizations induced by $GABA_A$ receptors; however, GABA application induced a transient inhibition of currents mediated by AMPA receptors in OPCs. These results indicate that OPCs are a direct target of interneuronal collaterals and that the GABA-induced Cl^- flux generated by these events may influence oligodendrocyte development by regulating the efficacy of glutamatergic signaling in OPCs.

Glia express receptors for many neurotransmitters[1], which enables neurons to communicate rapidly with surrounding glia and allows glia to assess the level of neuronal activity. This neuron-to-glia cell signaling influences the differentiation of glia progenitors[2,3], maintains astroglia ensheathment of synapses[4] and regulates the efficacy of inhibitory transmission[5]. Neurotransmitter receptors on glia have also been implicated in several human pathologies, as they regulate the growth and migration of gliomas[6] and predispose preterm infants to ischemia-induced damage to white matter[7]. The presence of receptors on glia represents an additional site of action for many therapeutics. Despite the universal expression of these receptors by glia and their demonstrated involvement in essential physiological processes, little is known about the patterns of neuronal activity that are necessary to elicit their activation *in situ* and the dynamics of receptor signaling that result. Such information is essential for understanding when these forms of signaling occur and how they influence the physiology of glia.

Direct communication between neurons and glia progenitor cells seems to be important for the continued generation of glia in the adult central nervous system, as neuronal activity and factors derived from neurons influence both the proliferation[8,9] and maturation of glia[2,3,8]. Studies of O-2A cells, glia that were initially isolated from optic nerve that develop into oligodendrocytes or "Type-2" astrocytes *in vitro*[10], showed that they express receptors for various neurotransmitters, including low-affinity α-amino-3-hydroxy-5-methyl isoxazole propionic acid (AMPA)[11,12] and γ-aminobutyric acid-A ($GABA_A$) receptors[13,14]. O-2A cells are antigenically and physiologically similar to OPCs, self-renewing glia progenitors that are found in both gray and white matter[15,16], raising the possibility that conventional neurotransmitters are used for rapid neuron–glia cell communication *in vivo*. The low affinity of these receptors and their presumed location remote from nerve terminals has raised questions, however, about how these receptors become activated.

Rapid and precise signaling between neurons is ensured by the distribution of receptor–ion channels in clusters at synapses, the rapid dilution of transmitter in the extracellular space, receptor desensitization and isolation through astroglia ensheathment[4] and through the activity of transporters[17]. Although transmitter can reach receptors on astroglia by spilling out of the synaptic cleft[18–20], such extrasynaptic signaling is necessarily slower, as it is constrained by the lower concentrations of transmitter achieved[21]. A recent study showed that pyramidal neurons form direct synapses with OPCs in the hippocampus[22], suggesting that neurons influence progenitor cell physiology through rapid activation of Ca^{2+}-permeable AMPA receptors. To determine whether GABAergic interneurons also communicate with OPCs through direct synapses, we recorded from OPCs in the hippocampus under conditions that were appropriate for GABA-mediated transmission. We found that spontaneous $GABA_A$ receptor–mediated currents with rapid kinetics occur in OPCs in the developing and adult hippocampus and that they exhibit properties consistent with release at direct interneuron–OPC synapses. These GABAergic responses regulate the efficacy of AMPA receptor currents in OPCs, and thus may influence their maturation into oligodendrocytes.

Department of Neuroscience, Johns Hopkins University School of Medicine, 725 N. Wolfe Street, WBSB 813, Baltimore, Maryland 21205, USA. Correspondence should be addressed to D.E.B. (dbergles@jhmi.edu).

Published online 7 December 2003; doi:10.1038/nn1162

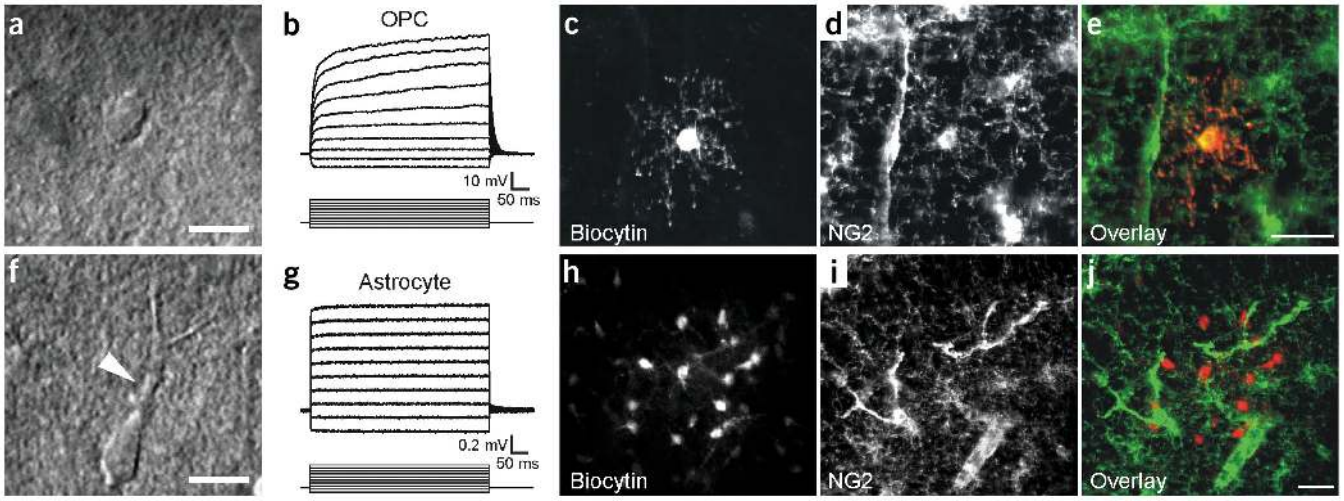

Figure 1 OPCs are inexcitable glial cells that are physiologically and morphologically distinct from astrocytes. (**a**) Infrared-DIC image of an OPC located in the stratum radiatum region of the hippocampus (P14 rat). Scale bar, 10 μm. (**b**) Whole-cell current-clamp recording from an OPC located in stratum radiatum of the hippocampus. Injection of positive current depolarized the cell but did not induce action potentials (steps: –60 to 300 pA,40 pA/step; KMeS-based electrode solution). (**c**) Morphology of a representative OPC that was filled with biocytin through the electrode. (**d**) NG2 immunoreactivity of the same region of the slice. (**e**) Overlay illustrating colocalization between biocytin and NG2, identifying this cell as an OPC. (**f**) Infrared-DIC image of an astrocyte located in the stratum radiatum region of the hippocampus (P14 rat). Arrowhead highlights the prominent process projecting from the cell body. Scale bar, 10 μm. (**g**) Current-clamp responses from a stratum radiatum astrocyte, illustrating the small change in membrane potential produced by the same current injection as in **b** (KMeS-based electrode solution). (**h**) Unlike OPCs, filling a single astrocyte with biocytin resulted in the labeling of many cells, because of diffusion of this marker through gap junctions. (**i**) NG2 immunoreactivity of the same region of the slice shown in **h**. (**j**) Overlay illustrating that physiologically identified astrocytes did not exhibit NG2 immunoreactivity (scale bars, 20 μm in **c**–**e**,**h**–**j**).

RESULTS

Identification of hippocampal OPCs

Putative OPCs in the stratum radiatum region of area CA1 were distinguished from interneurons by their smaller size and from astrocytes by their round soma and lack of visible processes (**Fig. 1a**,**f**). Cells with this morphology had higher input resistances than astrocytes (OPCs: 150 ± 12 MΩ, $n = 10$; astrocytes: 7 ± 1 MΩ, $n = 8$; $P < 0.01$; KMeS internal; **Fig. 1b**,**g**), but unlike neurons, they exhibited only small voltage-gated Na^+ currents (**Fig. 4a**,**b**). OPCs also did not exhibit large outward currents, which are characteristic of mature oligodendrocytes[23]. Fluorescent labeling of putative OPCs showed that they have numerous thin processes that radiate from a small cell body (**Fig. 1c**). Only a single cell was visible when recordings were made from one OPC, indicating that these cells were not extensively coupled by gap junctions, unlike physiologically identified astrocytes (**Fig. 1h**). Of the putative OPCs recovered after processing, 33 of 33 were immunoreactive for NG2 ($NG2^+$; **Fig. 1c**–**e**), a plasma membrane–associated sulfated proteoglycan that is expressed by OPCs[24]. In contrast, astrocytes were never $NG2^+$ (four of four groups of cells; **Fig. 1h**–**j**). Thus, OPCs can be reliably identified in acute brain slices by their unique morphological and electrophysiological properties.

$GABA_A$ receptor expression by OPCs

In vitro studies of O-2A progenitor cells have shown that they express ionotropic $GABA_A$ receptors[13,14]. To determine whether OPCs express functional $GABA_A$ receptors *in situ*, we measured their response to focal application of the selective $GABA_A$ receptor agonist 4,5,6,7-tetrahydroisoxazolo[5,4-c]pyridin-3-ol hydrochloride (THIP; 10 mM). Brief (3–7 ms) applications of THIP elicited currents in OPCs that reversed at 0 mV (–0.9 ± 1.3 mV, $n = 4$; CsCl internal) and were blocked by picrotoxin (100 μM) and SR-95531 (5 μM; $n = 4$; **Fig. 2a**). To confirm that these currents resulted from direct activation of $GABA_A$ receptors on OPCs, we removed outside-out patches from OPCs and measured their response to GABA. Brief (~1 ms) applications of a saturating dose of GABA (10 mM) to these patches elicited rapid inward currents that decayed bi-exponentially ($n = 6$) and were blocked by SR-95531 (**Fig. 2b**), indicating that functional $GABA_A$ receptors are expressed by OPCs.

Stimulus-evoked activation of $GABA_A$ receptors in OPCs

To determine if OPC $GABA_A$ receptors are activated by GABA that is released from interneurons, we examined whether these receptors were activated after stimulation of inhibitory afferents. In the absence of receptor antagonists, stimulation in stratum radiatum elicited a biphasic inward current in OPCs (CsCl internal; **Fig. 2c**). Much of the initial current was blocked by the AMPA/kainate receptor antagonist 2,3-dioxo-6-nitro-1,2,3,4-tetrahydrobenzo[f]quinoxaline-7-sulfonamide (NBQX; 5 μM), which is consistent with results described previously[22], whereas the slowly decaying current was blocked by subsequent application of SR-95531 (5 μM; $n = 8$; **Fig. 2d**). The partial inhibition of the slowly decaying current by NBQX was attributed to inhibition of polysynaptic excitation of interneurons (see **Supplementary Fig. 1** online). Evoked $GABA_A$ receptor responses in OPCs were dependent on both axonal conduction and Ca^{2+} influx, as they were blocked by tetrodotoxin (TTX; 1 μM; $n = 4$) or Cd^{2+} (30 μM $CdCl_2$; $n = 3$; **Fig. 2e**). In addition, OPC responses exhibited paired-pulse depression (paired-pulse ratio = 0.65 ± 0.06; $n = 7$), which is similar to evoked inhibitory postsynaptic currents (IPSCs) in pyramidal neurons.

Spontaneous $GABA_A$ receptor currents were also observed in OPCs in the absence of TTX (**Fig. 3a**). If these currents result from interneuronal activity, their frequency should be increased by carbachol, a muscarinic acetylcholine receptor agonist that potently depolarizes interneurons[25]. Indeed, the frequency of spontaneous $GABA_A$ receptor currents in OPCs was increased by 1240 ± 618% (range, 67–2,793%; $n = 5$) by carbachol (5 μM; **Fig. 3b**). This effect was inhibited by TTX

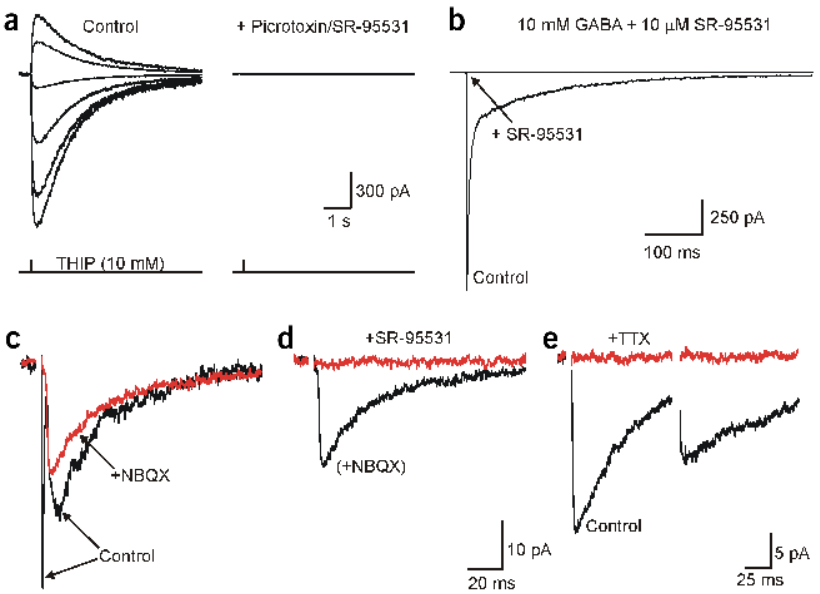

Figure 2 OPCs express functional $GABA_A$ receptors. (**a**) Focal application of 10 mM THIP (4 ms; bottom trace) near the cell body of an OPC in a hippocampal slice elicited transient currents that reversed near the predicted Cl^- reversal potential (E_{Cl-} = ~0 mV; steps: –30 to 20 mV, 10 mV/step) and were blocked by picrotoxin (100 μM) and SR-95531 (5 μM; CsCl-based electrode solution). (**b**) Brief (1 ms) application of GABA (10 mM) to an outside-out patch that was removed from the cell body of an OPC located in stratum radiatum elicited a transient inward current that was blocked by SR-95531, indicating expression of functional $GABA_A$ receptors (V_m = –70 mV; CsCl-based electrode solution). Electrical stimulation (30 μA, 100 μs, single pulse) of afferents in stratum radiatum elicited a biphasic inward current in a nearby OPC, which exhibited rapidly decaying and slowly decaying components. (**c**) The initial fast component was blocked by NBQX (5 μM; red trace), indicating that it was mediated by AMPA receptors. (**d**) The remaining slowly decaying component was blocked by SR-95531 (5 μM; red trace), indicating that it was mediated by $GABA_A$ receptors. Same scale in **c** and **d**. (**e**) The evoked release of GABA onto OPCs was also blocked by TTX (1 μM), indicating that it was dependent on action potential initiation. Evoked $GABA_A$ receptor currents in OPCs exhibited paired-pulse depression, which was similar to monosynaptic IPSCs recorded from pyramidal neurons. The ACSF for this experiment contained 5 μM NBQX and 5 μM RS-CPP.

(1 μM; n = 5), indicating that these carbachol-induced events required action potential–dependent release of transmitter. Carbachol did not alter the membrane potential of OPCs in perforated-patch recordings (**Supplementary Fig. 2** online), and depolarization of GABA-loaded OPCs did not induce auto-activation of $GABA_A$ receptors on these cells (**Supplementary Fig. 3** online), suggesting that this GABA was not released from OPCs[11]. Together, these results indicate that action potential initiation in local inhibitory interneurons leads to transient activation of $GABA_A$ receptors on OPCs.

Quantal release of GABA onto OPCs

To determine if direct GABAergic synapses are formed between interneurons and OPCs, we searched for the occurrence of miniature $GABA_A$ receptor currents in whole-cell recordings from OPCs (in TTX). OPCs were distinguished from neurons and astrocytes based on their response to step depolarization (**Fig. 4a,b**). In ACSF containing TTX and NBQX, slowly decaying spontaneous currents occurred in OPCs at a low frequency (1 to <0.01 Hz; **Fig. 4c,e,g**). These currents were potentiated by pentobarbital, an anesthetic that increases the open time of $GABA_A$ receptors (amplitude increased by 19 ± 12%, P = 0.23; τ, the decay time constant, increased by 158 ± 11%, P = 0.03; n = 3) and were blocked by SR-95531 (5 μM; n = 10), indicating that they resulted from the transient activation of $GABA_A$ receptors. Application of SR-95531 did not alter the baseline noise or holding current in OPCs (n = 4 cells; data not shown), indicating that these receptors may not be subject to tonic activation.

Ruthenium red increases the frequency of miniature IPSCs (mIPSCs) in CA1 pyramidal neurons without changing their amplitude[26]. Application of ruthenium red (100 μM) similarly increased the frequency of $GABA_A$ currents in OPCs by three- to fourfold but did not alter their amplitudes or kinetics (data not shown), which allowed us to acquire more events for analysis. The amplitudes of these miniature $GABA_A$ receptor–mediated currents varied over a wide range (average amplitude = –14.8 ± 0.9 pA, n = 17; V_m = –70 mV) but could be as large

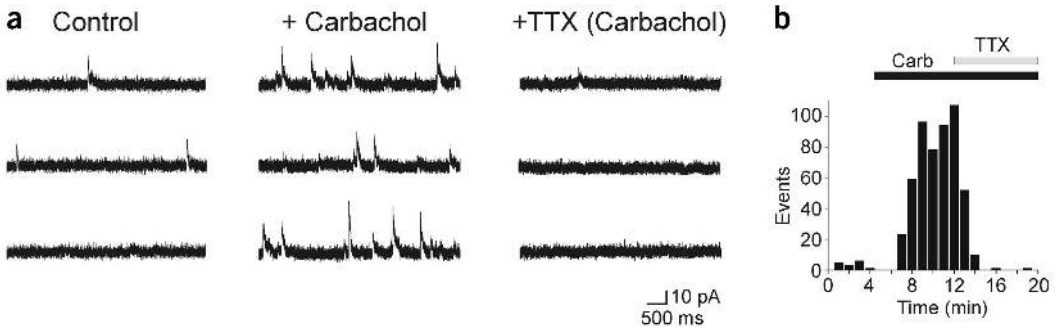

Figure 3 Increasing the firing rate of local interneurons increases the frequency of spontaneous $GABA_A$ receptor currents in OPCs. (**a**) Spontaneous $GABA_A$ receptor currents recorded from an OPC. $GABA_A$ receptor currents are outward because a CsMeS-based electrode solution was used and the cell was held at +30 mV to increase the driving force and improve the signal-to-noise level. Bath application of carbachol (5 μM), which potently depolarizes interneurons, increased the frequency of these events. The carbachol-induced increase in spontaneous events was blocked by TTX (1 μM). Each set of sweeps represents a continuous time period. The ACSF contained 5 μM NBQX. (**b**) Plot of the frequency of $GABA_A$ receptor currents over time for this experiment.

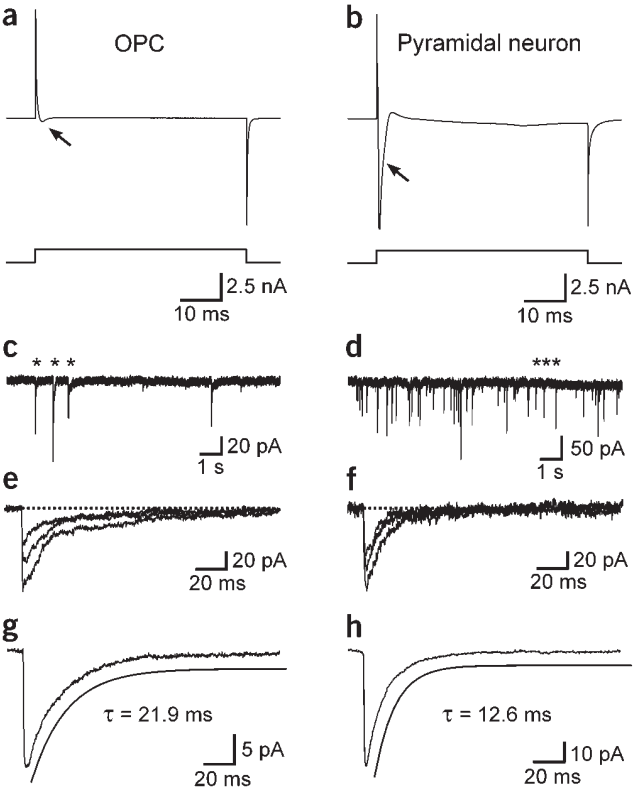

Figure 4 Miniature $GABA_A$ receptor–mediated currents occur in OPCs. (**a**) Depolarization of an OPC to –20 mV (from –70 mV) elicited only a small inward current (arrow). (**b**) Step depolarization of a CA1 pyramidal neuron, however, elicited a large inward Na^+ spike (arrow; CsCl-based electrode solution in **a** and **b**). (**c**) Spontaneous inward currents were observed in OPCs in the presence of TTX (1 μM) and NBQX (5 μM). (**d**) They occurred at a higher frequency in pyramidal neurons. (**e**) Overlay of three spontaneous currents (indicated by asterisks in **c**), illustrating the slow decay kinetics of $GABA_A$ receptor responses in this OPC. (**f**) Overlay of three spontaneous currents (indicated by asterisks in **d**) recorded from this pyramidal neuron. (**g**) Average time course of 64 events recorded from this OPC. (**h**) Average time course of 108 mIPSCs recorded from this pyramidal neuron. The decay time was ~50% faster than that observed for $GABA_A$ receptor currents recorded from OPCs. (**a**,**c**,**e**,**g** were recorded from one OPC, and **b**,**d**,**f**,**h** were recorded from one CA1 pyramidal neuron.) Recordings were carried out in hippocampal slices from P14 animals.

as –75 pA. These currents rose rapidly (0.81 ± 0.06 ms) but decayed slowly (τ = 23.6 ± 0.7 ms, $n = 17$; **Fig. 4g**). By comparison, GABAergic mIPSCs recorded from CA1 pyramidal neurons under similar conditions were larger (average amplitude = –44.5 ± 2.2 pA, $n = 7$; $P < 0.001$) and decayed about twice as fast (τ = 13.6 ± 0.5 ms, $n = 7$; $P < 0.001$; **Fig. 4d, f, h**). The occurrence of miniature $GABA_A$ receptor events in OPCs indicates that the amount of GABA contained in a single synaptic vesicle is sufficient to induce rapid activation of these OPC receptors.

OPC GABA responses arise from direct synaptic release

The $GABA_A$ receptor currents observed in OPCs could arise from the direct release at interneuron–OPC synapses, spillover from synapses formed between neurons, or through nonsynaptic mechanisms such as reversal of GABA transporters. Responses dependent on spillover are often enhanced by inhibiting transporter-dependent uptake[17]. However, the kinetics of miniature OPC $GABA_A$ receptor currents recorded at 36 °C were not altered by SKF 89976-A (SKF), a nonsubstrate antagonist of GABA transporters ($\tau_{SKF}/\tau_{control}$ = 1.13 ± 0.09, $n = 4$; $P = 0.12$; **Fig. 5a**), although SKF 89976-A decreased their amplitudes ($amplitude_{SKF}/amplitude_{control}$ = 0.79 ± 0.06, $n = 5$; $P < 0.05$). The decrease in amplitude of these events may reflect a partial desensitization of $GABA_A$ receptors because of an increase in ambient GABA[27]. Transporter inhibition also had little effect on evoked responses ($\tau_{SKF}/\tau_{control}$ = 1.07 ± 0.11, $n = 6$; $P = 0.45$; **Fig. 5b**). In addition, raising the temperature from 22–24 °C to 35–37 °C, a manipulation that was expected to increase the cycling rate of GABA transporters and reduce spillover, increased the amplitude of miniature $GABA_A$ receptor responses in OPCs by 40 ± 12% ($P = 0.03$) and decreased their decay times by 62 ± 3.0% ($n = 4$; $P < 0.001$; **Fig. 5c**). This treatment did not, however, prevent the occurrence of these currents. The changes in

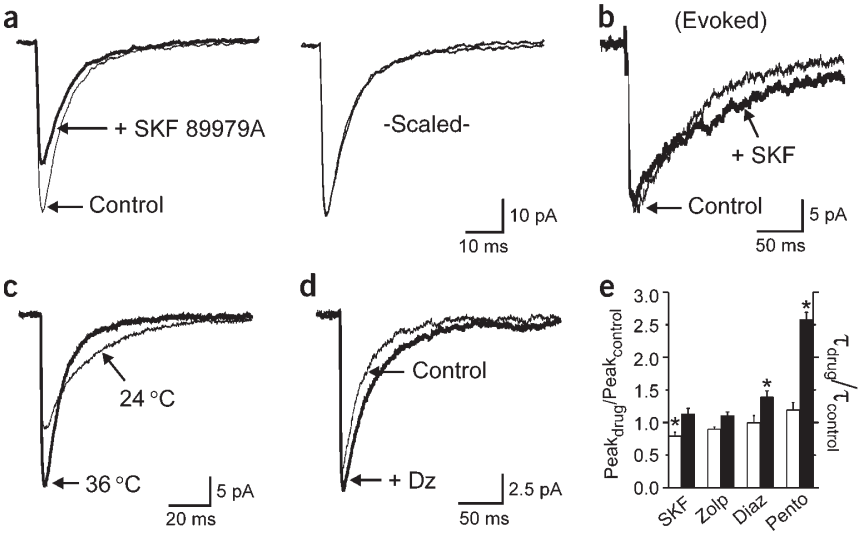

Figure 5 $GABA_A$ receptor currents in OPCs arise from direct interneuron–OPC synapses. (**a**) Average time course of $GABA_A$ receptor currents recorded from an OPC under control conditions (thin trace, 65 events) and in the presence of the GABA transporter inhibitor SKF 89976A (100 μM; thick trace, 67 events). At right, the two average waveforms are scaled. Recordings were made at 36° C. (**b**) Evoked $GABA_A$ receptor currents recorded from an OPC in control and in SKF 89976A (100 μM). (**c**) Average time course of spontaneous miniature $GABA_A$ receptor currents recorded from an OPC at room temperature (24 °C, thin trace; 64 events) and 36 °C (thick trace; 77 events). (**d**) Average waveform of spontaneous miniature $GABA_A$ receptor currents recorded in control conditions (thin trace, 141 events) or in the presence of diazepam (Dz; 10 μM; thick trace, 326 events). (**e**) Grouped data illustrating the effect of $GABA_A$ receptor modulators on the kinetics of miniature $GABA_A$ receptor currents recorded from OPCs. Open bars correspond to the ratio of the peak amplitude in control to that in drug, and filled bars correspond to the ratio of the τ decay of responses in drug to control (SKF, 100 μM SKF 89976A; Zolp, 10 μM zolpidem; Diaz, 10 μM diazepam; Pento, 50 μM pentobarbital). Asterisks denote a significant difference from control ($P < 0.05$). The ACSF for all experiments contained 5 μM NBQX and 5 μM RS-CPP, and all experiments except those in **b** were done in 1 μM TTX.

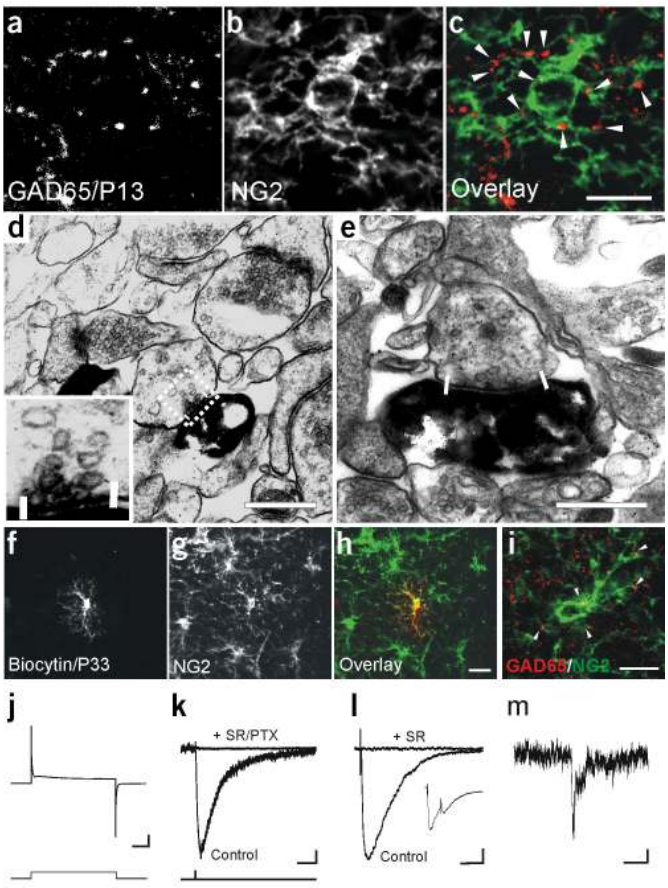

Figure 6 Morphological evidence for synaptic junctions between OPCs and interneurons. (**a**) GAD 65 immunoreactivity in the stratum radiatum region (P13 rat). (**b**) NG2 immunoreactivity of the same region shown in **a**. (**c**) Overlay showing close association of some GAD 65$^+$ puncta (red, arrowheads) with OPC processes (green). Scale bar, 10 μm. (**d**) Electron micrograph showing a process of an OPC (black, peroxidase) in apposition with a putative inhibitory nerve terminal. Inset shows area delineated by dashed rectangle. (**e**) A second example of a putative synaptic junction between an OPC and a nerve terminal. White bars in **d** and **e** highlight areas of contact. Scale bar, 0.4 μm in **d**,**e**. (**f**) Morphology of an adult hippocampal OPC (P33 rat). (**g**) NG2 immunoreactivity of the same region of the slice. (**h**) Overlay illustrating NG2 expression by this OPC. Scale bar, 20 μm. (**i**) Close association between NG2$^+$ processes (green) and GAD 65$^+$ puncta (red, arrowheads; P30 rat). Scale bar, 10 μm. (**j**) Step response (from –70 to –20 mV) of cell shown in **f**. Scale: 1 nA, 10 ms. (**k**) Response to 10 mM THIP for this OPC was blocked by SR-95531 (SR; 5 μM) and picrotoxin (PTX; 100 μM). Scale: 25 pA, 1 s. (**l**) Evoked $GABA_A$ receptor current from an adult OPC exhibited paired-pulse depression (inset). Scale: 20 pA, 100 ms (inset scale: 50 pA, 200 ms). (**m**) Spontaneous $GABA_A$ receptor current recorded from an adult OPC. Scale: 5 pA, 100 ms.

kinetics of these responses presumably result from an increase in unitary conductance and faster gating at higher temperatures.

Agents that increase receptor affinity enhance spillover responses to a greater extent than responses mediated by direct release[21], because the transmitter concentration experienced by receptors during spillover is much lower. Zolpidem, a benzodiazepine that increases the affinity of $GABA_A$ receptors[28], has been used to assess the occupancy of $GABA_A$ receptors in many neurons[28,29]. It was not possible to use zolpidem to probe the occupancy of OPC receptors, as it did not significantly alter miniature $GABA_A$ receptor currents in OPCs ($amplitude_{zolpidem}/amplitude_{control} = 0.90 \pm 0.03$, $P = 0.1$; $\tau_{zolpidem}/\tau_{control} = 1.11 \pm 0.06$, $P = 0.2$; $n = 3$; **Fig. 5e**), although it increased the amplitude and prolonged the decay of mIPSCs in pyramidal neurons (see also ref. 29; $amplitude_{zolpidem}/amplitude_{control} = 1.21 \pm 0.06$, $P = 0.1$; $\tau_{zolpidem}/\tau_{control} = 1.68 \pm 0.08$, $P < 0.01$; $n = 3$). These results suggest that OPC $GABA_A$ receptors have a different subunit composition. As an alternative, we examined the effect of diazepam, which similarly increases the affinity of $GABA_A$ receptors[30] and has been used to assess receptor occupancy at synapses[31]. Diazepam prolonged the decay of miniature $GABA_A$ receptor responses in OPCs but did not significantly alter their amplitudes ($\tau_{diazepam}/\tau_{control} = 1.39 \pm 0.09$, $P = 0.03$; $amplitude_{diazepam}/amplitude_{control} = 1.00 \pm 0.05$, $P = 0.94$; $n = 4$; **Fig. 5d**,**e**). Diazepam had similar effects on mIPSCs in CA1 pyramidal neurons ($amplitude_{diazepam}/amplitude_{control} = 1.00 \pm 0.11$, $P = 0.38$; $\tau_{diazepam}/\tau_{control} = 1.43 \pm 0.20$, $P = 0.05$; $n = 4$). The rapid onset of OPC miniature $GABA_A$ receptor currents, the lack of potentiation of these currents after inhibition of GABA transporters and the modest effect of increasing $GABA_A$ receptor affinity on their amplitudes are inconsistent with responses produced by spillover of GABA. These data indicate that $GABA_A$ receptors on OPCs are exposed to a brief, high-concentration transient of GABA, which is similar to that achieved within the synaptic cleft.

Morphological evidence of direct interneuron–OPC synapses

To determine if interneurons form direct synaptic junctions with OPCs, we examined whether inhibitory terminals are in contact with OPC processes. GAD 65$^+$ puncta were observed in close apposition to NG2$^+$ processes of OPCs in the stratum radiatum region (**Fig. 6a–c**); a similar colocalization was observed for 30 NG2$^+$ cells in eight slices. Furthermore, electron microscopic analysis of slices in which physiologically identified OPCs had been loaded with biocytin, showed that nerve terminals containing pleomorphic vesicles, which is characteristic of vesicles containing GABA, were in direct contact with OPC processes (**Fig. 6d**,**e**). These data indicate that the quantal $GABA_A$ receptor currents observed in OPCs may be generated at direct synaptic junctions between interneurons and OPCs.

GABAergic synapses on adult OPCs

Although the number of NG2$^+$ progenitors declines from the early postnatal period to adulthood, NG2$^+$ cells remain abundant in the adult brain[16]. To determine whether synapses also are present between interneurons and NG2$^+$ OPCs in the mature brain, we recorded from OPCs in hippocampal slices prepared from adult rats. Putative OPCs in these slices had morphological and physiological properties that were similar to those in younger animals (**Fig. 6j**), and four of four cells that were recovered after tissue processing were NG2$^+$ (**Fig. 6f–h**). Similar to young animals, GAD 65$^+$ puncta were also observed in close proximity to NG2$^+$ processes at this age (**Fig. 6i**). Focal application of THIP to these cells elicited inward currents that were blocked by SR-95531 and picrotoxin ($n = 5$; **Fig. 6k**), and stimulation in stratum radiatum elicited transient inward currents in the presence of NBQX that exhibited paired-pulse depression (P2/P1 = 0.42 ± 0.26, $n = 4$) and were blocked by SR-95531 ($n = 4$; **Fig. 6l**). Furthermore, spontaneous inward currents were observed in all of these cells ($n = 8$), which had kinetics similar to those recorded from OPCs in slices prepared from young animals (**Fig. 6m**). These results indicate that GABAergic signaling in OPCs is not restricted to early developmental periods.

GABA depolarizes OPCs

Activation of $GABA_A$ receptor–ion channels can induce either a depolarization or hyperpolarization, depending on the intracellular

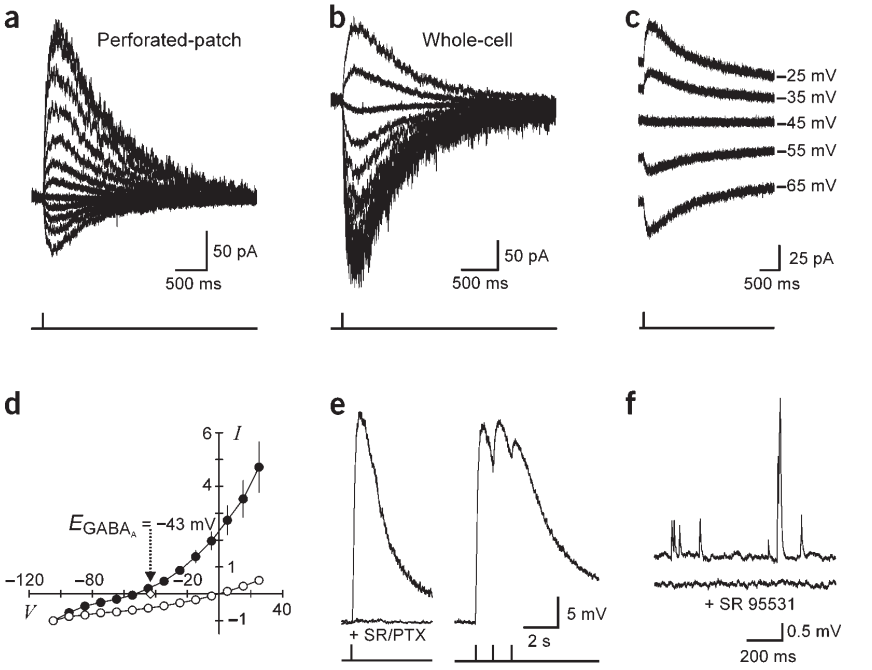

Figure 7 OPCs have high $[Cl^-]_i$ and are depolarized by GABA. (**a**) Responses of an OPC to focal application of 10 mM THIP recorded in the gramicidin perforated-patch configuration. The cell was held at potentials between –100 and +30 mV. (**b**) Response of the cell in **a** after rupture of the patch and internal dialysis with Cl^- (CsCl-based electrode solution). (**c**) Response of an OPC to application of THIP recorded near the predicted reversal potential for the current ($E_{GABA\text{-}A}$). (**d**) Plot of the average peak amplitudes (normalized) of responses at different voltages in perforated-patch (filled circles) or whole-cell (open circles) recording configurations. The reversal potential of $GABA_A$ receptor responses was determined to be –43 mV (diamond). (**e**) Focal application of 10 mM THIP depolarized an OPC ~30 mV from the resting potential (V_m = –99 mV). Repeated application of THIP did not depolarize this cell further. These responses were blocked by SR-95531 (SR; 10 μM) and picrotoxin (PTX; 100 μM). (**f**) Spontaneous $GABA_A$ receptor–mediated depolarizations recorded from an OPC after bath application of carbachol (5 μM; V_m = –99 mV). These transient depolarizing potentials were blocked by SR-95531 (5 μM), indicating that they were mediated by $GABA_A$ receptors (gramicidin perforated-patch current-clamp recording). The ACSF in **a**–**f** contained 5 μM NBQX and 5 μM RS-CPP, and in **a**–**e** contained 1 μM TTX.

concentration of Cl^- ($[Cl^-]_i$). If $[Cl^-]_i$ is high, as it is in immature neurons[32] and cultured glial cells[33], opening of $GABA_A$ receptor–channels leads to Cl^- efflux and depolarization. To determine the physiological reversal potential of $GABA_A$ currents ($E_{GABA\text{-}A}$) in OPCs, we recorded THIP responses in perforated-patch recordings from OPCs using gramicidin-A[34]. THIP-evoked currents in OPCs reversed at –43.6 ± 2.3 mV (CsCl; n = 7; **Fig. 7a**,**c**,**d**), which was not significantly different when methanesulfonate was used as the primary anion in the perforated-patch solution ($E_{GABA\text{-}A}$ = –42.9 ± 6.4 mV, n = 3; P = 0.92), a manipulation that would have shifted the reversal to more hyperpolarized potentials if this anion had been able to diffuse into the cell. In pyramidal neurons, THIP-evoked responses reversed at –73.0 ± 1.4 mV (n = 6; P < 0.001), indicating that OPCs maintain a higher $[Cl^-]_i$ than mature neurons. In several recordings, we were able to destroy the perforated patch with further suction, establishing a conventional whole-cell recording; for OPCs, the reversal potential shifted to –0.9 ± 1.3 mV (CsCl internal; n = 4; **Fig. 7b**,**d**), and for neurons the reversal potential shifted to –3.5 ± 1.5 mV (CsCl internal; n = 4), indicating that the integrity of the perforated patch was maintained prior to rupture. Based on this reversal potential, OPCs have a calculated $[Cl^-]_i$ of ~21 mM, whereas the calculated $[Cl^-]_i$ for pyramidal neurons at this age was ~4 mM.

In perforated-patch recordings, the resting potential of OPCs in hippocampal slices was –102.5 ± 0.6 mV (n = 4), which is close to the calculated reversal potential for K^+ (E_K = –102.3 mV), suggesting that activation of $GABA_A$ receptors would induce a depolarization. Indeed, focal application of THIP depolarized OPCs by 29.0 ± 2.9 mV (n = 4) in current clamp (gramicidin perforated patch; **Fig. 7e**). This depolarization seemed to be maximal, because repeated applications of THIP did not result in further depolarization. In the presence of carbachol, transient $GABA_A$ receptor–mediated depolarizations of OPCs were visible in all cells (n = 4) in perforated-patch recordings, the largest of which were ~5 mV in amplitude (**Fig. 7f**). These results indicate that action potential initiation in interneurons induces a transient depolarization of OPCs resulting from Cl^- efflux though $GABA_A$ receptors.

GABA modulation of glutamate receptor currents

The very negative resting potential of OPCs and the small depolarization produced by GABA raises questions about the physiological role of this GABAergic signaling. GABA exerts potent inhibitory effects on neurons by increasing the membrane conductance (shunting) and by hyperpolarizing the resting membrane potential. Application of GABA to OPCs elicited a similar increase in conductance (**Fig. 8a**), which decreased the amplitude of AMPA receptor currents that were evoked by focal application of kainate by 49.1 ± 8.1% (n = 5; **Fig. 8b**–**d**). In addition, GABA application produced a transient inhibition of AMPA receptor currents that persisted after GABA was removed and the membrane conductance had returned to control values, similar to an effect described previously in motor neurons[35]. These results indicate that GABA may act to limit AMPA receptor signaling in OPCs by increasing the membrane conductance and by altering intracellular Cl^-.

DISCUSSION

In this study, we examined the mechanisms responsible for activation of $GABA_A$ receptors in OPCs, a population of glia progenitors found throughout the developing and adult nervous system[24]. We show that GABA released from interneurons causes rapidly activating currents in OPCs, indicating that these receptors are transiently exposed to a high concentration of GABA. The features of these quantal GABA responses were consistent with phasic rather than spillover-mediated transmission[36], suggesting that OPCs are a direct target of interneuron collaterals. The direct synaptic activation of $GABA_A$ and AMPA[22]

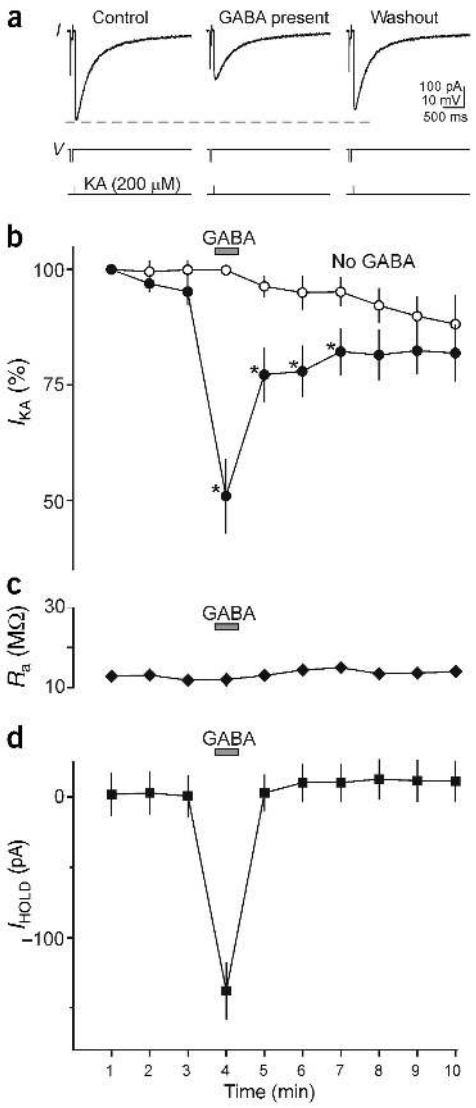

Figure 8 GABA inhibits AMPA receptor currents in OPCs. (**a**) Perforated-patch recording from an OPC (P14 rat) showing representative responses (upper traces) elicited by a 4-ms puffer application of kainate (KA, 200 μM; lower traces) with a KCl-based internal solution (V_m = −100 mV). GABA (5 mM) was applied for 40 s by bath application. The middle traces show the duration of the voltage step (50 ms, −5 mV) that was applied (visible just before kainate response) to assess access resistance and membrane conductance. (**b**) Plot of the average peak amplitude of kainate-evoked responses (I_{KA}) for experiments when GABA was applied (n = 5) and when GABA was not applied (n = 4). Asterisks represent significant (P < 0.05) differences between the peak amplitude of responses. (**c**) Plot of the average access resistance (R_a) over the duration of the recordings shown in **b**. (**d**) Plot of the average holding current (I_{hold})over the duration of the recordings shown in **b**. All recordings were done in the presence of 1 μM TTX and 5 μM RS-CPP.

receptors in OPCs provides a mechanism for rapid neuron–glia communication in the hippocampus.

Properties of OPC $GABA_A$ receptors

Quantal $GABA_A$ receptor currents recorded in OPCs occurred at a lower frequency, were smaller in amplitude and decayed more slowly than mIPSCs recorded from CA1 pyramidal neurons at this age. The slower decay of these currents can be attributed to differences in subunit composition. Miniature IPSCs in many neurons exhibit a similarly slow decay early in development; the transition to faster decay kinetics has been attributed to an increase in α1-containing receptors[37,38] and is accompanied by a corresponding increase in sensitivity to zolpidem. OPC $GABA_A$ receptors were insensitive to zolpidem but were sensitive to diazepam, a pharmacological profile characteristic of α5-containing receptors[39]. In OPCs, these receptors are subject to direct activation, whereas in neurons most α5-containing receptors are thought to be located extrasynaptically[40]. The expression of α5-containing receptors by OPCs raises the possibility that OPCs may be involved in the cognitive enhancements seen in α5 knockout mice[41].

GABA receptor signaling in glia

Although many glial cells express GABA receptors[5,42], there have been few reports describing activation of these receptors after neuronal stimulation. Interneuronal stimulation leads to activation of $GABA_B$ receptors on astrocytes, resulting in a slow rise in $[Ca]_i$ (ref. 5). This rise in $[Ca]_i$ triggers a glutamate release that ultimately acts on receptors in inhibitory nerve terminals to potentiate GABA release. The high affinity of these metabotropic $GABA_B$ receptors presumably allows them to respond to spillover of GABA from synapses. Stimulation of hypothalamic afferents in a pituitary preparation induces a biphasic response in astroglia-like stellate cells that is mediated by $GABA_A$ and D2 dopamine receptors[43]. $GABA_A$ receptor activation in these cells induces a transient depolarization that is similar to the one observed in OPCs, although it has much slower kinetics (stellate cell: rise time, >20 ms; decay time, >100 ms versus OPC: rise time, <5 ms; decay time, <30 ms for current-clamp recordings). These responses were attributed to direct release of GABA onto stellate cells at "synaptoid" contacts[44] rather than through spillover. However, the large number of fibers activated during stimulation, the presence of rapid $GABA_A$ receptor currents in adjacent melanotrophs, the slow kinetics of the response and uncertainties about the identity of the neurotransmitter present at synaptoid contacts make it difficult to distinguish between these two possibilities. Nevertheless, the results presented here, and additional anatomical evidence that neurons form defined synaptic junctions with glia[22,44], indicate that direct synaptic signaling between neurons and glia may be more widespread than has been appreciated.

Functions of $GABA_A$ receptor signaling in OPCs

Oligodendrocyte development is regulated by factors secreted from neurons[2], and neurotransmitters such as glutamate[3] and ATP[22] inhibit the proliferation of OPCs and promote their differentiation into oligodendrocytes *in vitro*. Furthermore, GABA influences the proliferation, migration and differentiation of neural progenitors[32]. The diverse effects of GABA are mediated primarily by $GABA_A$ receptors, which are expressed before synapse formation. Like OPCs, immature neurons maintain a high $[Cl^-]_i$ (ref. 45), and $GABA_A$ receptor activation depolarizes these cells and increases $[Ca^{2+}]_i$ by activating voltage-gated Ca^{2+} channels. Such GABA-driven activity alters gene expression and morphogenesis[45] and is essential for the maturation of neurons[35]. Many inputs would have to be simultaneously active, however, to force the membrane potential of OPCs close to the range for activation for Ca^{2+} channels, because their resting potential is 20–30 mV more negative than neurons. Indeed, the maximal depolarization produced by THIP was not sufficient to trigger a rise in $[Ca^{2+}]_i$ in OPCs (data not shown), indicating that GABA may exert its effects through other means. Application of GABA increased the membrane conductance of OPCs and decreased the size of AMPA receptor currents evoked by kainate by inducing a shunting inhibi-

tion. This GABA-induced inhibition persisted for several minutes after washout of GABA, however, indicating that GABA may also negatively regulate AMPA receptors by lowering intracellular Cl^-. Notably, a GABA-induced rise in intracellular Cl^- potentiates AMPA receptor currents in spinal motor neurons[8]. Rapid $GABA_A$ receptor signaling in OPCs through direct neuron–glia synapses may thus allow interneurons to influence the physiology and, perhaps, fate of OPCs in the developing and mature nervous system.

METHODS

Slice preparation. We prepared hippocampal slices from young postnatal (P13–16) or older (P33–60) Sprague-Dawley rats as described previously[22], in accordance with a protocol approved by the Animal Care and Use Committee at Johns Hopkins University. Slices were maintained in artificial cerebral spinal fluid (ACSF): 119 mM NaCl, 2.5 mM KCl, 2.5 mM $CaCl_2$, 1.3 mM $MgCl_2$, 1 mM NaH_2PO_4, 26.2 mM $NaHCO_3$ and 11 mM glucose. Slices from older animals were cut using a sapphire blade in a solution containing 110 mM choline chloride, 25 mM $NaHCO_3$, 25 mM D-glucose, 11.6 mM sodium ascorbate, 7 mM $MgSO_4$, 3.1 mM sodium pyruvate, 2.5 mM KCl, 1.25 mM NaH_2PO_4 and 0.5 mM $CaCl_2$. Slices were maintained thereafter in ACSF. The ACSF was bubbled with 95% O_2/5% CO_2, and unless noted, all experiments were carried out at 22–24 °C. We used infrared light on an upright microscope (Zeiss Axioskop FS2) equipped with differential interference contrast (DIC) optics and a CCD (charge-coupled device) camera (Sony XC-73) to visualize the OPCs.

Electrophysiology. We made whole-cell recordings from OPCs using conventional techniques[22]. The internal solution consisted of 130 mM CsCl, 20 mM HEPES, 10 mM EGTA, 2 mM Na-ATP and 0.2 mM Na-GTP, pH 7.3. In some experiments, KCl, KCH_3SO_3H (KMeS) or $CsCH_3SO_3H$ (CsMeS) was substituted for CsCl, as noted. Evoked responses were elicited with a constant-current stimulator using a bipolar electrode (stimulus: 30–100 μA, 100 μs). Pipette resistances were 2–4 MΩ, and recordings were made without series resistance compensation. Membrane potentials have been corrected for liquid junction potentials. For experiments involving diazepam, we included the carrier (ethanol, 3.3 mM) in control and diazepam solutions. We made perforated-patch recordings with an internal solution containing 5 μg/ml gramicidin-A. $GABA_A$ receptors were activated by THIP through pressure application using a Picospritzer II (Parker Hannifin) in TTX (1 μM), NBQX (5 μM) and (*RS*)-3-(2-carboxypiperazin-4-yl)-propyl-1-phosphonic acid (RS-CPP; 5 μM). Nucleated outside-out patches were removed from OPCs and rapid solution changes were made using a piezoelectric bimorph. The external solution for the patch experiments contained 135 mM NaCl, 2.5 mM KCl, 2.5 mM $CaCl_2$, 1.3 mM $MgCl_2$ and 20 mM HEPES, pH 7.4.

Analysis. Currents and potentials were recorded using an Axopatch 200B or Axopatch 1D amplifier (Axon Instruments), filtered at 2–5 kHz and digitized at 50 kHz using pClamp8 (Axon Instruments). Data were analyzed off-line using Clampfit (Axon Instruments), Origin (OriginLab) and Mini analysis (Synaptosoft) software. Data are expressed as mean ± s.e.m., and statistical significance was determined using the paired or unpaired Student's *t*-test. The paired-pulse ratio was determined by dividing the average peak amplitude of the second response by the peak amplitude of the first response. We have truncated stimulus artifacts for clarity. The intracellular concentration of Cl^- was calculated from the measured reversal potential for GABA using $E_{GABA\text{-}A} = (RT/F)/\ln[([Cl^-]_e + 0.2[HCO_3^-]_e)/([Cl^-]_i + 0.2[HCO_3^-]_i)]$, as described[46].

Histology. We filled OPCs with biocytin (0.15%) and fixed them in 4% paraformaldehyde in PBS with 0.1% picric acid overnight at 4 °C. Slices were resectioned, extracted with 0.3% Triton X-100 and blocked with 5% donkey serum. NG2 was detected with a rabbit anti-rat NG2 antibody (1:1,000; generously provided by W.B. Stallcup, Burnham Institute)[47]; this antibody labels OPCs as well as smooth muscle cells and pericytes surrounding capillaries. NG2 immunoreactivity was detected with Cy2-conjugated anti-rabbit IgG, and biocytin was visualized with Cy5-conjugated streptavidin (both at 1:500; Jackson ImmunoResearch). For dual NG2/GAD 65 labeling, NG2 was detected with a guinea pig anti-NG2 antibody (1:1,000; gift of W.B. Stallcup) and Cy3-conjugated donkey anti-guinea pig secondary (1:500; Jackson ImmunoResearch), whereas GAD 65 (1:500; rabbit, Sigma) was detected with a Cy2-conjugated donkey anti-rabbit IgG secondary (1:500; Jackson ImmunoResearch). Fluorescence images were collected with a Noran Oz confocal microscope (Noran) using Kr-Ar (488 nm, 568 nm) and red HeNe (633 nm) lasers, FITC (500–550 nm band-pass), rhodamine (578–633 nm band-pass) and Cy5 filter sets (660 nm low-pass). Control hippocampal sections incubated with secondary antibody alone did not produce labeling. For electron microscopy, slices containing physiologically identified OPCs were fixed and processed as described[22].

Note: Supplementary information is available on the Nature Neuroscience website.

ACKNOWLEDGMENTS

We thank C. Jahr for support during the initial part of this work, P. Somogyi and J.D.B. Roberts for their help with electron microscopy and S.H. Kong for help with cryosectioning. Supported by the Sloan Foundation and a Basil O'Connor Scholar Award from the March of Dimes Foundation.

COMPETING INTERESTS STATEMENT

The authors declare that they have no competing financial interests.

Received 15 September; accepted 14 November 2003
Published online at http://www.nature.com/natureneuroscience/

1. Barres, B.A., Chun, L.L. & Corey, D.P. Ion channels in vertebrate glia. *Annu. Rev. Neurosci.* **13**, 441–474 (1990).
2. Yuan, X., Eisen, A.M., McBain, C.J. & Gallo, V. A role for glutamate and its receptors in the regulation of oligodendrocyte development in cerebellar tissue slices. *Development* **125**, 2901–2914 (1998).
3. Stevens, B., Porta, S., Haak, L.L., Gallo, V. & Fields, R.D. Adenosine: a neuron-glia transmitter promoting myelination in the CNS in response to action potentials. *Neuron* **36**, 855–868 (2002).
4. Iino, M. *et al.* Glia-synapse interaction through Ca^{2+}-permeable AMPA receptors in Bergmann glia. *Science* **292**, 926–929 (2001).
5. Kang, J., Jiang, L., Goldman, S.A. & Nedergaard, M. Astrocyte-mediated potentiation of inhibitory synaptic transmission. *Nat. Neurosci.* **1**, 683–692 (1998).
6. Takano, T. *et al.* Glutamate release promotes growth of malignant gliomas. *Nat. Med.* **7**, 1010–1015 (2001).
7. Follett, P.L., Rosenberg, P.A., Volpe, J.J. & Jensen, F.E. NBQX attenuates excitotoxic injury in developing white matter. *J. Neurosci.* **20**, 9235–9241 (2000).
8. Barres, B.A. & Raff, M.C. Proliferation of oligodendrocyte precursor cells depends on electrical activity in axons. *Nature* **361**, 258–260 (1993).
9. Gallo, V. *et al.* Oligodendrocyte progenitor cell proliferation and lineage progression are regulated by glutamate receptor-mediated K^+ channel block. *J .Neurosci.* **16**, 2659–2670 (1996).
10. Raff, M.C., Miller, R.H. & Noble, M. A glia progenitor cell that develops in vitro into an astrocyte or an oligodendrocyte depending on culture medium. *Nature* **303**, 390–396 (1983).
11. Barres, B.A., Koroshetz, W.J., Swartz, K.J., Chun, L.L. & Corey, D.P. Ion channel expression by white matter glia: the O-2A glia progenitor cell. *Neuron* **4**, 507–524 (1990).
12. Patneau, D.K., Wright, P.W., Winters, C., Mayer, M.L. & Gallo, V. Glial cells of the oligodendrocyte lineage express both kainate- and AMPA-preferring subtypes of glutamate receptor. *Neuron* **12**, 357–371 (1994).
13. Von Blankenfeld, G., Trotter, J. & Kettenmann, H. Expression and developmental regulation of a $GABA_A$ receptor in cultured murine cells of the oligodendrocyte lineage. *Eur. J. Neurosci.* **3**, 310–316 (1991).
14. Williamson, A.V., Mellor, J.R., Grant, A.L. & Randall, A.D. Properties of $GABA_A$ receptors in cultured rat oligodendrocyte progenitor cells. *Neuropharmacology* **37**, 859–873 (1998).
15. Levison, S.W., Young, G.M. & Goldman, J.E. Cycling cells in the adult rat neocortex preferentially generate oligodendroglia. *J. Neurosci. Res.* **57**, 435–446 (1999).
16. Chang, A., Nishiyama, A., Peterson, J., Prineas, J. & Trapp, B.D. NG2-positive oligodendrocyte progenitor cells in adult human brain and multiple sclerosis lesions. *J. Neurosci.* **20**, 6404–6412 (2000).
17. Isaacson, J.S., Solis, J.M. & Nicoll, R.A. Local and diffuse synaptic actions of GABA in the hippocampus. *Neuron* **10**, 165–175 (1993).
18. Clark, B.A. & Cull-Candy, S.G. Activity-dependent recruitment of extrasynaptic NMDA receptor activation at an AMPA receptor-only synapse. *J. Neurosci.* **22**, 4428–4436 (2002).
19. Bergles, D.E., Dzubay, J.A. & Jahr, C.E. Glutamate transporter currents in bergmann glial cells follow the time course of extrasynaptic glutamate. *Proc. Natl. Acad. Sci. USA* **94**, 14821–14825 (1997).
20. Porter, J.T. & McCarthy, K.D. Hippocampal astrocytes in situ respond to glutamate released from synaptic terminals. *J. Neurosci.* **16**, 5073–5081 (1996).

21. Dzubay, J.A. & Jahr, C.E. The concentration of synaptically released glutamate outside of the climbing fiber-Purkinje cell synaptic cleft. *J. Neurosci.* **19**, 5265–5274 (1999).
22. Bergles, D.E., Roberts, J.D., Somogyi, P. & Jahr, C.E. Glutamatergic synapses on oligodendrocyte precursor cells in the hippocampus. *Nature* **405**, 187–191 (2000).
23. Steinhauser, C., Berger, T., Frotscher, M. & Kettenmann, H. Heterogeneity in the membrane current pattern of identified glial cells in the hippocampal slice. *Eur. J. Neurosci.* **4**, 472–484 (1992).
24. Levine, J.M., Reynolds, R. & Fawcett, J.W. The oligodendrocyte precursor cell in health and disease. *Trends Neurosci.* **24**, 39–47 (2001).
25. Pitler, T.A. & Alger, B.E. Cholinergic excitation of GABAergic interneurons in the rat hippocampal slice. *J. Physiol.* **450**, 127–142 (1992).
26. Sciancalepore, M., Savic, N., Gyori, J. & Cherubini, E. Facilitation of miniature GABAergic currents by ruthenium red in neonatal rat hippocampal neurons. *J. Neurophysiol.* **80**, 2316–2322 (1998).
27. Overstreet, L.S., Jones, M.V. & Westbrook, G.L. Slow desensitization regulates the availability of synaptic $GABA_A$ receptors. *J. Neurosci.* **20**, 7914–7921 (2000).
28. Perrais, D. & Ropert, N. Effect of zolpidem on miniature IPSCs and occupancy of postsynaptic $GABA_A$ receptors in central synapses. *J. Neurosci.* **19**, 578–588 (1999).
29. Hajos, N., Nusser, Z., Rancz, E.A., Freund, T.F. & Mody, I. Cell type- and synapse-specific variability in synaptic $GABA_A$ receptor occupancy. *Eur. J. Neurosci.* **12**, 810–818 (2000).
30. Lavoie, A.M. & Twyman, R.E. Direct evidence for diazepam modulation of $GABA_A$ receptor microscopic affinity. *Neuropharmacology* **35**, 1383–1392 (1996).
31. Frerking, M., Borges, S. & Wilson, M. Variation in GABA mini amplitude is the consequence of variation in transmitter concentration. *Neuron* **15**, 885–895 (1995).
32. Owens, D.F., Boyce, L.H., Davis, M.B. & Kriegstein, A.R. Excitatory GABA responses in embryonic and neonatal cortical slices demonstrated by gramicidin perforated-patch recordings and calcium imaging. *J. Neurosci.* **16**, 6414–6423 (1996).
33. Gilbert, P., Kettenmann, H. & Schachner, M. Gamma-aminobutyric acid directly depolarizes cultured oligodendrocytes. *J. Neurosci.* **4**, 561–569 (1984).
34. Ebihara, S., Shirato, K., Harata, N. & Akaike, N. Gramicidin-perforated patch recording: GABA response in mammalian neurones with intact intracellular chloride. *J. Physiol.* **484**, 77–86 (1995).
35. Van Damme, P., Callewaert, G., Eggermont, J., Robberecht, W. & Van Den Bosch, L. Chloride influx aggravates Ca^{2+}-dependent AMPA receptor-mediated motoneuron death. *J. Neurosci.* **23**, 4942–4950 (2003).
36. Mody, I. Distinguishing between $GABA_A$ receptors responsible for tonic and phasic conductances. *Neurochem. Res.* **26**, 907–913 (2001).
37. Cohen, A.S., Lin, D.D. & Coulter, D.A. Protracted postnatal development of inhibitory synaptic transmission in rat hippocampal area CA1 neurons. *J. Neurophysiol.* **84**, 2465–2476 (2000).
38. Goldstein, P.A. *et al.* Prolongation of hippocampal miniature inhibitory postsynaptic currents in mice lacking the $GABA_A$ receptor alpha1 subunit. *J. Neurophysiol.* **88**, 3208–3217 (2002).
39. Burgard, E.C., Tietz, E.I., Neelands, T.R. & Macdonald, R.L. Properties of recombinant gamma-aminobutyric acid A receptor isoforms containing the alpha 5 subunit subtype. *Mol. Pharmacol.* **50**, 119–127 (1996).
40. Brunig, I., Scotti, E., Sidler, C. & Fritschy, J.M. Intact sorting, targeting, and clustering of gamma-aminobutyric acid A receptor subtypes in hippocampal neurons *in vitro*. *J. Comp. Neurol.* **443**, 43–55 (2002).
41. Collinson, N. *et al.* Enhanced learning and memory and altered GABAergic synaptic transmission in mice lacking the alpha 5 subunit of the $GABA_A$ receptor. *J. Neurosci.* **22**, 5572–5580 (2002).
42. Pastor, A., Chvatal, A., Sykova, E. & Kettenmann, H. Glycine- and GABA-activated currents in identified glial cells of the developing rat spinal cord slice. *Eur. J. Neurosci.* **7**, 1188–1198 (1995).
43. Mudrick-Donnon, L.A., Williams, P.J., Pittman, Q.J. & MacVicar, B.A. Postsynaptic potentials mediated by GABA and dopamine evoked in stellate glial cells of the pituitary pars intermedia. *J. Neurosci.* **13**, 4660–4668 (1993).
44. Theodosis, D.T. & MacVicar, B. Neurone-glia interactions in the hypothalamus and pituitary. *Trends Neurosci.* **19**, 363–367 (1996).
45. Ganguly, K., Schinder, A.F., Wong, S.T. & Poo, M. GABA itself promotes the developmental switch of neuronal GABAergic responses from excitation to inhibition. *Cell* **105**, 521–532 (2001).
46. Staley, K.J., Soldo, B.L. & Proctor, W.R. Ionic mechanisms of neuronal excitation by inhibitory $GABA_A$ receptors. *Science* **269**, 977–981 (1995).
47. Tillet, E., Ruggiero, F., Nishiyama, A. & Stallcup, W.B. The membrane-spanning proteoglycan NG2 binds to collagens V and VI through the central nonglobular domain of its core protein. *J. Biol. Chem.* **272**, 10769–10776 (1997).